Final version submitted to Estuarine, Coastal and Shelf Sciences 11.1.2018

Accepted 14.1.2018

Nitrification and the ammonia-oxidizing communities in the central Baltic Sea water column

Running head: Nitrification in the central Baltic Sea

Helena Jäntti[1*], Bess B. Ward[2], Joachim W. Dippner[3], Susanna Hietanen[4]

[1]University of Helsinki, Department of Environmental Sciences, Division of Aquatic Sciences, P.O. Box 65, 00014 University of Helsinki, Finland. helena.jantti@uef.fi

[2]Princeton University, Department of Geosciences, 217 Guyot Hall, Princeton, NJ 08544, United States. bbw@princeton.edu

[3]Leibniz Institute for Baltic Sea Research Warnemünde, Department of Biological Oceanography, Seestrasse 15, D-18119 Rostock, Federal Republic of Germany. joachim.dippner@io-warnemuende.de

[4]University of Helsinki, Department of Environmental Sciences, Division of Aquatic Sciences, P.O. Box 65, 00014 University of Helsinki, Finland. susanna.hietanen@helsinki.fi

[*]Corresponding author. Current address: University of Eastern Finland, Department of Environmental and Biological Sciences, P.O. Box 1627, 70211 Kuopio, Finland.

Key words: Ammonia-oxidizing bacteria, ammonia-oxidizing archaea, microarray, nitrification, Baltic Sea

Abstract

The redoxclines that form between the oxic and anoxic water layers in the central Baltic Sea are sites of intensive nitrogen cycling. To gain better understanding of nitrification, we measured the biogeochemical properties along with potential nitrification rates and analyzed the assemblages of ammonia-oxidizing bacteria and archaea using functional gene microarrays. To estimate nitrification in the entire water column, we constructed a regression model for the nitrification rates and applied it to the conditions prevailing in the area in 2008-2012. The highest ammonia oxidation rates were found in a thin layer at the top of the redoxcline and the rates quickly decreased below detection limit when oxygen was exhausted. This is probably because extensive suboxic layers, which are known to harbor pelagic nitrification, are formed only for short periods after inflows in the Baltic Sea. The nitrification rates were some of the highest measured in the water columns, but the thickness of the layer where conditions were favorable for nitrification, was very small and it remained fairly stable between years. However, the depth of the nitrification layer varied substantially between years, particularly in the eastern Gotland Basin (EGB) due to turbulence in the water column. The ammonia oxidizer communities clustered differently between the eastern and western Gotland Basin (WGB) and the composition of ammonia-oxidizing assemblages correlated with the environmental variables. The ammonia oxidizer community composition was more even in the EGB, which may be related to physical instability of the redoxcline that does not allow predominance of a single archetype, whereas in the WGB, where the position of the redoxcline is more constant, the ammonia-oxidizing community was less even. Overall the ammonia-oxidizing communities in the Baltic Sea redoxclines were very evenly distributed compared to other marine environments where microarrays have been applied previously.

1. Introduction

The Baltic Sea is one of the largest brackish water basins (415 200 km^2) in the world and subject to severe eutrophication (HELCOM 2009). The high nutrient load from the drainage basin and salinity stratification caused by positive freshwater balance have led to formation of widespread anoxic areas in the deep basins, which are separated by sills that prevent an even flow of water to the bottom areas. The widest anoxic basin in the central Baltic Sea is the Gotland Deep and the deepest the Landsort Deep (Figure 1). These basins are characterized by suboxic transition zones, redoxclines, which form in the area between the oxygenated surface and the euxinic bottom water. Unlike in many other oxygen deficient zones (ODZ), the redoxcline intermittently disappears in the central Baltic Sea due to inflow of saline ($\geq$17) and oxygen rich water from the North Sea through the Danish Straits. During such events, termed as Major Baltic Inflows (MBI), the sulfidic water in the bottom of the deepest basins is replenished with oxygen (O_2) and the redoxcline disappears. MBIs occur mainly during winter and since the mid-1970s the frequency of MBIs has decreased to almost decadal, which has led to a long-term stagnation and made anoxia a nearly permanent feature of the central Baltic Sea (Schinke and Matthäus, 1998). In addition to MBIs, there is also smaller scale mixing in the water column which occurs during stagnation. The drivers for the small scale mixing are not well understood, but they are in general a result of complex hydrodynamic processes such as upwelling, boundary mixing, Kelvin-Helmholtz and other shear instabilities and internal wave breakings (Zhurbas and Paka, 1999, Kuzmina *et al.*, 2005, Reissmann *et al.*, 2009, van der Lee and Umlauf 2011).

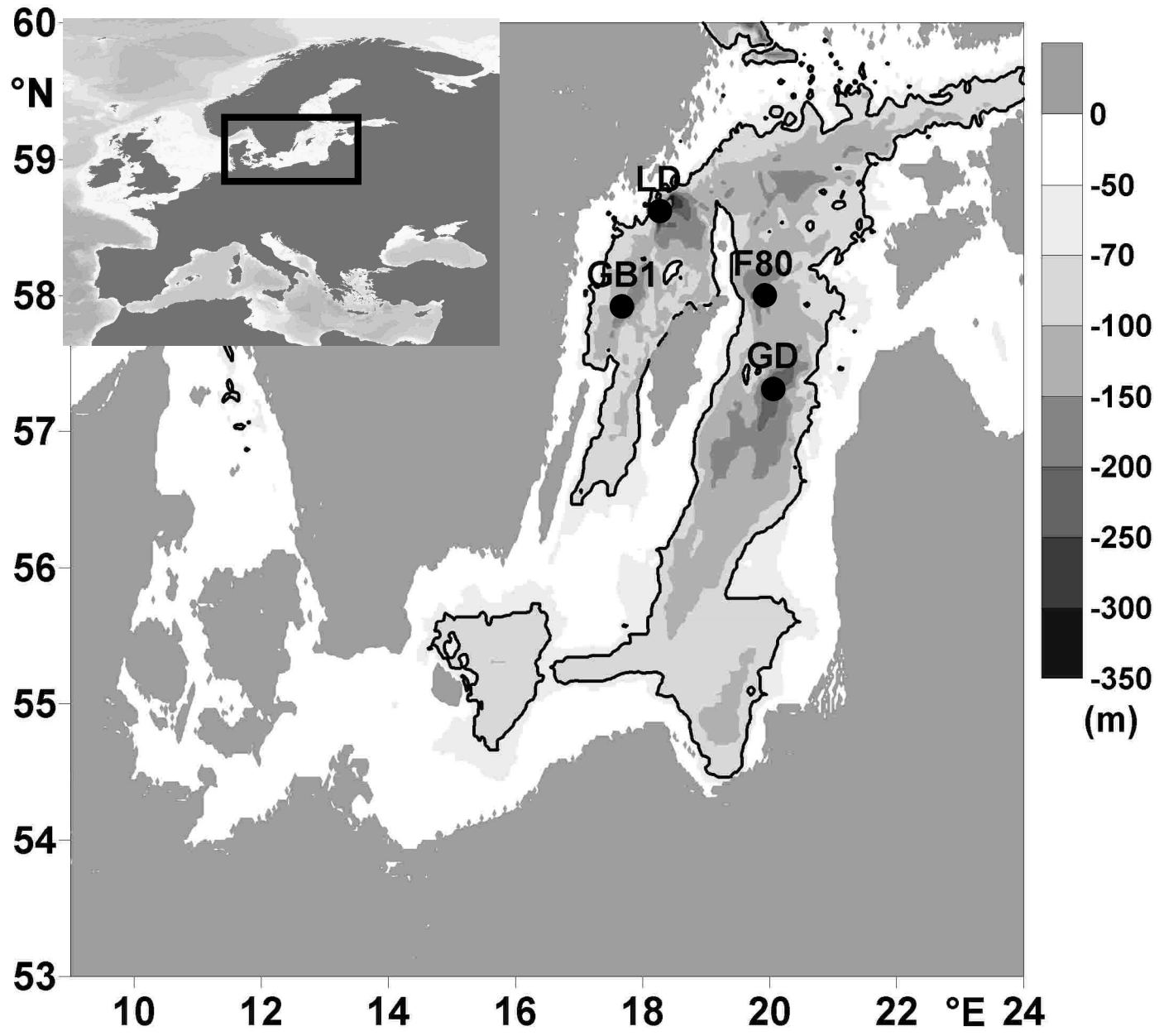

Figure 1. Topography of the Baltic Proper and the position of the sampling stations (LD, GB1, GD, and F80). GD is located in the Eastern Gotland Basin, LD and GB1 in the Western Gotland Basin and F80 in the Farö deep. The full line marks the 70 m depth contour, which encloses the area of hypoxic water.

ODZs have received a lot of interest because they are nitrogen cycling hotspots. In the Baltic Sea, a substantial portion of the nitrogen (N) entering the area is converted from reactive forms to dinitrogen gas (N_2) via pelagic denitrification (Rönner, 1983; Rönner and Sörensson, 1985; Brettar and Rheinheimer, 1991; Hannig *et al.*, 2007; Hietanen *et al.*, 2012; Dalsgaard *et al.*, 2013, Bonaglia *et al.*, 2016). Globally, 30–50%

of the total nitrogen (N) loss in the oceans occurs in the ODZs (Codispoti *et al.*, 2011). Nitrification, which supplies the electron acceptor for denitrification, has also been measured at high rates in the ODZs. In the Baltic Sea Enoksson (1986) found potential nitrification up to 280 nmol N L^{-1} d^{-1} in a station south-west from for the island of Gotland, with the highest rates occurring below the halocline. However, the rate estimate may be hindered by bottle effects (i.e. senescence of cell material, which may increase the availability of ammonium, (NH_4^+)) because the incubations lasted considerably longer than measurements done with modern, more sensitive isotopic ratio mass spectrometers (IRMS). Bauer (2003) measured potential nitrification rates of 202 nmol N L^{-1} d^{-1} in the Gotland Deep and in more recent measurements, Hietanen *et al.* (2012) found potential nitrification rates of up to 160 nmol N L^{-1} d^{-1} in the Landsort Deep and Berg *et al.* (2015) 130 nmol N L^{-1} d^{-1} in the Gotland Deep. Rates this high in marine water columns have been detected previously only in the periodically hypoxic Bornholm Deep in the southern Baltic Sea (883.8 nmol N L^{-1} d^{-1}; Berg *et al.*, 2015), in the Peruvian oxygen minimum zone (144 nmol N L^{-1} d^{-1}; Lam *et al.*, 2009), and in the Saanich Inlent (319 nmol L^{-1} d^{-1}; Grundle and Juniper, 2011).

Both archaeal and bacterial ammonia oxidizers can be active in ODZs. In the early 2000s, when the existence of ammonia-oxidizing archaea (AOA) was unknown, the ammonia-oxidizing community in the central Baltic Sea water column was suggested to be composed of β-proteobacteria (Bauer, 2003). Later on when AOA were discovered, the ammonia-oxidizing community in the central Baltic Sea was suggested to consist mainly of one thaumarchaeotal subcluster closely related to *Candidatus* Nitrosopumilus maritimus (Labrenz *et al.*, 2010, Berg *et al.*, 2015). In the northern Baltic Sea sediments, the ammonia oxidizer communities had surprisingly low diversity and were dominated by organisms with gene signatures unique to the sampling area (Vetterli *et al.*, 2016). Hence, the ammonia-oxidizing communities in the Baltic Sea appear to have a low diversity and harbor unique species, but the overall community composition and its controlling factors are still largely unknown.

105 The diversity and community composition of ammonia oxidizers can be investigated using functional gene
106 microarrays that are designed to specifically target the ammonia-oxidizing bacteria (AOB) and AOA, using
107 sequences of their *amoA* genes, which encode ammonia monooxygenase subunit A. Since ammonia
108 oxidizers are metabolically restrained, there is very little divergence of essential genes and consequently the
109 diversity of ammonia oxidizers is relatively limited. All AOB and AOA sequences known at the time of
110 these experiments (2010–2011), both cultivated and environmental, could be targeted with this method. Each
111 microarray contains a set of archetype probes that are selected from the entire database of homologous
112 sequences, using an algorithm (Bulow *et al.*, 2008) that is similar to that used to select operational taxonomic
113 units (OTUs) (e.g. program for Defining Operational Taxonomic Units and Estimating Species Richness
114 (DOTUR); Schloss and Handelsman, 2005). Thus, each archetype represents all sequences within 85%
115 identity with the probe sequence, and the comparisons between the samples are made on the basis of relative
116 rather than absolute sequence identity because the intensity of the hybridization signal cannot be interpreted
117 quantitatively (Ward *et al.*, 2007).

118 We determined the spatial variation in the ammonia-oxidizing communities at three sites in the central Baltic
119 Sea redoxclines, using functional microarrays, to investigate how ammonia oxidizer communities are
120 composed in dynamic redoxcline where salinity and O_2 concentration in the nitrification layer change
121 frequently. We also measured the nitrification rates at four sites, created a regression model for nitrification
122 and applied it to the high resolution monitoring data that was in the IOW molecular database to estimate the
123 spatial and temporal variation of the pelagic nitrification. Thereafter, we tested whether composition of the
124 ammonia-oxidizing community correlates with the potential nitrification rates, environmental conditions
125 prevailing in the sampled areas and depths, and the differences in the hydrodynamic patterns between the
126 sampling sites. Finally, since there is interest on the pelagic denitrification and anammox due to their
127 capability to mitigate the effects of the excess N loading, we estimated how efficiently nitrification supplies
128 electron acceptors for the N_2 producing processes in this system.

Materials and methods

2.1. Sample collection

The samples for the nitrification rate measurements were collected from four stations during three cruises 2010-2011 (Table 1). Station GB1 is located at the western Gotland Basin (WGB), station LD at the Landsort Deep, station GD at them Eastern Gotland Basin (EGB), and station F80 at the Fårö Deep (Figure 1). The microarray samples were collected in 2010 from GB1, GD, and LD (Table 1). At each of the sampling stations, the salinity, temperature, and O_2 profiles were first determined, using a CTD (conductivity-temperature-depth) profiler with an attached SBE43 O_2 sensor (both SeaBird Electronics Inc, Bellevue, WA, USA). The oxic-anoxic interface was identified as the depth at which the signal of the O_2 sensor began to increase when the sensor was pulled slowly upwards after a short period on the anoxic side of the redoxcline. After determining the O_2 profiles, the water samples were collected near the oxic-anoxic boundary in Niskin bottles using a CTD-rosette system. Once the bottles were on deck, samples were taken from two replicate bottles for potential nitrification rate measurement, microarray (only in 2010), nutrient analyses (NO_3^-, NO_2^-, and NH_4^+; detection limits 0.01 µmol L^{-1}, 0.01 µmol L^{-1}, and 0.3 µmol L^{-1}, respectively), O_2 (Winkler titration, detection limit 0.89 µmol L^{-1}), and H_2S (detection limit 0.02 µmol L^{-1}). The nutrient, O_2 and H_2S analyses followed the protocol by Grasshoff *et al.* (1983).

Table 1. The sampling stations and times, bottom and sample depths, O_2, H_2S, NO_3^-, NO_2^-, and NH_4^+ concentrations, and potential nitrification rates. B/D stands for below detection limit and SE for standard error.

Station	sampling month/ year	depth (m) bottom	depth (m) sample	O_2 µmol L^{-1}	H_2S µmol L^{-1}	NO_3^- µmol L^{-1}	NO_2^- µmol L^{-1}	NH_4^+ µmol L^{-1}	Potential nitrification rate nmol N L^{-1} d^{-1} (SE)	Microarray sample (Yes/No)
GB1	6/2010	147	57	68.3	B/D	4.70	0.03	0.5	10.1 (1.9)	Yes
	6/2010		60	49.1	B/D	4.71	0.05	0.4	11.0 (0.7)	No
	6/2010		63	20.5	B/D	4.40	B/D	0.2	31.3 (4.23)	No
	5/2011		70	12.0	B/D	4.47	0.03	0.2	30.6 (5.2)	No
	5/2011		75	0.01	B/D	0.05	B/D	2.0	1.0 (0.4)	No
LD	6/2010	453	70	4.9	B/D	2.34	0.04	0.3	79.3 (13.6)	Yes
	6/2010		73	B/D	B/D	0.45	B/D	1.6	B/D	No
	6/2010		76	3.1	4.5	0.14	B/D	3.0	5.4 (1.0)	No
	5/2011		68	9.4	B/D	5.04	0.03	B/D	22.7 (8.5)	No
	5/2011		72	1.3	B/D	0.85	1.24	1.2	81.2 (19.3)	No
GD	7/2010	242	120	0.1	B/D	4.10	0.03	B/D	75.5 (8.9)	No
	7/2010		123	1.8	B/D	B/D	B/D	0.6	3.9 (1.1)	Yes
	7/2010		126	4.5	B/D	B/D	B/D	1.3	B/D	Yes
	7/2010		130	B/D	14.2	B/D	B/D	2.9	B/D	No
	5/2011		132	B/D	9.4	1.66	0.68	0.2	43.2 (11.5)	No
	7/2011		117	5.8	B/D	5.68	0.01	B/D	14.3 (4.3)	No
	7/2011		118	7.6	B/D	5.96	0.01	B/D	B/D	No
	7/2011		119	7.1	B/D	4.41	0.06	B/D	B/D	No
F80	5/2011	191	116	0.9	B/D	1.87	0.15	0.1	B/D	No
	5/2011		120	0.9	B/D	3.47	0.06	0.2	2.2 (0.4)	No

2.2. Potential nitrification rate measurements

The potential nitrification rates were estimated by measuring the production of $^{15}NO_2^-$ and $^{15}NO_3^-$ in samples that were amended with excess $^{15}NH_4^+$. This was done by transferring a water sample from the Niskin bottle into glass bottles with a threefold overflow, and adding ^{15}N-labelled ammonium chloride ($^{15}NH_4Cl$, 99% ^{15}N, Sigma Aldrich, St. Louis, MO, USA; final concentration ~5 µM resulting in atom enrichment of 63-99-atom%) to the samples under a dinitrogen (N_2) atmosphere. The samples were then divided into 20-mL glass vials (n = nine per treatment) sealed gastight with butyl rubber stoppers and aluminum crimps and incubated in the dark at near *in situ* temperature (~5 °C). For each sample depth, three replicate samples were filtered approximately every 3−4 h through prewashed 0.2 µm syringe filters (polyethylsulfone [PES] membrane; VWR International LLC, Radnor, PA, USA) to terminate the incubation. The maximum incubation time of the samples was approximately 9 h. The filtered samples were frozen at -20 °C for later $^{15}NO_3^-$ and $^{15}NO_2^-$ (hereafter referred to as $^{15}NO_x^-$) analysis.

The $^{15}NO_x^-$ contents of the potential nitrification rate samples were analyzed using the denitrifer method (Sigman *et al.*, 2001) with small modifications. *Pseudomonas chlororaphis* (American Type Culture Collection (ATCC) 13985) was grown in an 800-mL liquid culture (tryptic soy broth; Fluka Analytical (Sigma-Aldrich Chemie GmbH), Buchs, Switzerland), 10 mM potassium nitrate (KNO_3), 1 mM ammonium sulfate ($(NH_4)_2SO_4$), and 1 mL L^{-1} antifoaming agent (Dow Corning Antifoam RD emulsion; Midland, MI, USA)) on a shaker table (150 rotations per minute) for 8 d in the dark at room temperature. Thereafter, the bacterial culture was concentrated 10-fold by centrifugation and the concentrated culture was divided into 2-mL aliquots in 12-mL gastight glass vials (Exetainer; Labco Ltd, Lampeter, Ceredigion, UK). The vials were closed and purged with N_2 for 5 h. A sample amount corresponding to 8 nmol NO_x^- was injected into each vial and after overnight incubation in the dark, 0.1 mL of 10-M sodium hydroxide (NaOH) was injected into each vial to lyse the bacteria and strip the CO_2 from the headspace to the liquid. When the sample was too diluted (less than 8 nmol of NO_x^- in 5 mL), a 5-mL sample was injected into the vials to determine whether

minimum detectable amount (~1 nmol) of nitrous oxide (N_2O) would form. The ^{15}N label in the N_2O produced from NO_x^- by the denitrifying bacteria was analyzed with a gas chromatographic isotope ratio mass spectrometer (GC-IRMS) system (Thermo Finnigan Delta V plus with ConFlo IV; Thermo Fisher Scientific, Waltham, MA, USA) with a trace gas preconcentrator (PreCon; Thermo Fisher Scientific) in the Department of Environmental Science, University of Eastern Finland, Kuopio.

2.3. Microarray analyses of the amoA gene

The samples for the microarray analyses were collected in 2010 from one depth at GB1 and LD and from two depths at GD at the same time as the nitrification rate samples (Table 1). For each sample (n = two per sampling depth), 1.5 L of water were filtered through a 0.22-µm pore-size nitrocellulose membrane filter (diameter 47 mm, Durapore®; Millipore, Billerica, MA, USA) with gentle vacuum. The filters were then packed in microcentrifuge tubes and frozen immediately at -70 °C for later analysis. In the laboratory, the DNA from the samples was extracted, using the Qiagen Allprep kit (Qiagen, Venlo, the Netherlands) and digested, using 50 ng of Hinf I restriction enzyme. Two sets of archetype probes were designed, using an established algorithm (Bulow *et al.*, 2008): one for AOB (30 probes, representing 502 sequences in GenBank in 2004) and a separate probe set for AOA (31 probes representing 1329 archaeal *amoA* sequences from GenBank in November 2008). The resolution of the array format is about 87% +/- 3% (Taroncher-Oldenburg *et al.*, 2003). Each 90-mer oligonucleotide probe consisted of a 70-mer archetype sequence combined with a 20-mer reference oligo as an internal standard. Targets for microarray hybridization were prepared, hybridized in duplicate on the microarray slide, and washed as described in Ward and Bouskill (2011). The washed slides were scanned, using a laser scanner 4200 (Agilent Technologies, Palo Alto, CA, USA) and analyzed with GenePix Pro 6.0 (Molecular Devices, Sunnyvale, CA, USA). All of the original array files are available at GEO (Gene Expression Omnibus; http://www.ncbi.nlm.nih.gov/geo/) at NCBI (National Center for Biotechnology Information) under GEO Accession No. GSE50164.

196 Quantification of the hybridization signals was performed according to Ward and Bouskill (2011). The initial
197 data are in the form of a fluorescence ratio (FR), the cyanine 3/cyanine 5 (Cy3/Cy5) ratio, for every feature.
198 The FR values were converted to a relative fluorescence ratio (RFR), which is the fraction of total
199 fluorescence (sum of all the FR values for each probe set) for each probe. Hence, the final results are relative
200 hybridization strengths, not absolute abundances.

201 ### 2.4. Calculations and statistical analyses

202 The potential nitrification rate was calculated by plotting the change in average NO_x^- concentrations over the
203 incubation time (Jäntti *et al.*, 2013). The slope of this equation represents the nitrification rate and the rate
204 was determined as significant when in linear regression analysis $P < 0.05$. The change in the NO_x^-
205 concentration for each time point was calculated according to equation 1:

206 (1) $$NO_x^- = [NO_x^-] \times (\Delta atom\%/100)/ R_{NH4}^+$$

207 where Δatom% is the difference between the atom% of NO_x^- at the time point and in the beginning of the
208 incubation and R_{NH4}^+ is the ^{15}N enrichment in the NH_4^+ pool after the addition of $^{15}NH_4^+$. To extrapolate the
209 potential nitrification rates for the entire central Baltic Sea, the rates and the environmental variables from
210 this study and Hietanen *et al.*, (2012) were combined and a stepwise multiple regression analysis was
211 performed with Sigmaplot statistic program (Systat, San Jose, CA, USA). The rates measured in zero O_2
212 concentration were excluded from the regression analysis due to high variability of rates that was probably
213 caused by some of the samples having H_2S and O_2 below the detection limit of the Winkler method. To
214 calculate the nitrification rates in the redoxcline, the regression model was applied to three independent data
215 sets collected in 2009, 2010, and 2011 by Frey *et al.*, (2014), where the O_2 and dissolved inorganic nitrogen
216 (DIN) concentrations were analyzed with a high vertical resolution in the central Baltic Sea. To extrapolate
217 the rates for the entire central Baltic Sea, the thickness and the depth of the active nitrification layer was

218 calculated from the IOW molecular biological data base, which contains vertically highly resolved DIN and
219 O_2 data collected from the central Baltic Sea during five IOW monitoring cruises 2008-2012 (FS Maria S.
220 Merian 08, June and August 2008; FS Alkor 332, February-March 2009; FS Maria S, Merian 12, August-
221 October 2009; FS Meteor 86, November-December 2011; FS Meteor 87, May-August 2012). The thickness
222 and the depth of the nitrification layer for each cruise was computed with gradient method by restricting the
223 NO_3^- concentration between 0-6.0 µM, O_2 concentration between 0-25.0 µmol L^{-1} and NH_4^+ concentration
224 between 0-1.0 µM. These concentration limits were chosen because in the Baltic Sea H_2S typically
225 accumulates almost immediately beneath the water layer where O_2 concentrations is below detection limit,
226 and inspection of the profiles showed that the NO_3^- peak, which is considered to be at the top of the active
227 nitrification layer, typically falls between these limits. Also, the highest ammonia oxidizer gene activity has
228 been shown to fall in between these limits (Labrenz *et al.* 2010). A careful inspection of the position of the
229 anoxic layer indicated that the 70 m depth contour is representative for the area of redoxcline. The area
230 surrounded by the 70 m depth contour was computed using the Matlab (Mathworks Natick, MA, USA)
231 function trapz(x,y), which provides a trapezoidal numerical integration of data with non-uniform spacing,

232 The diversity of the microbial communities was estimated by calculating the Shannon evenness index. The
233 Bray-Curtis dissimilarity index was calculated, using R (R Core Team 2012). Redundancy analysis (RDA)
234 was performed in R, using the RFR of each archetype (after square-root transformation) as the response
235 variables, and dissolved O_2, NO_3^-, and NH_4^+ concentrations and potential nitrification rates (at the microarray
236 sample depth) as explanatory variables.

237 # 3. Results

238 ## 3.1. The environmental conditions during nitrification rate measurements

239 The oxic-anoxic interface was between 70–126 m and mixing of oxic and euxinic water masses was evident
240 on some occasions at GD and LD where both H_2S and O_2 existed in the same water layers (Table 1). The O_2
241 concentration in the sampling depths was 0–70 µM, NH_4^+ concentration 0–3 µM and NO_3^- concentration 0–6
242 µM (Table 1). Substantial NO_2^- accumulation was observed only on few sampling occasions (Table 1).

243 ### 3.2. Nitrification rates

244 The highest potential nitrification rates (76−81 nmol N L^{-1} d^{-1}) were measured at stations GD and LD at
245 depths where O_2 was still present, but at low concentrations (Table 1). The NO_x^- concentration did not
246 increase linearly over the incubation period in 73 m at LD; in 126 m, 130 m, 118m, and 119 m at GD; and in
247 116 m at F80 (Table 1). Data from these measurements were discarded from further analyses. The non-
248 linearity was most likely caused by the low nitrification rates approaching the detection limit of the method.

249 The highest significant ($p = 0.0008$) R-value (0.6917) in the regression analysis was obtained for the
250 equation where logarithmic potential nitrification rate had a quadratic relationship with the logarithmic O_2
251 concentration (Equation 2, Figure 2).

252 (2) $\log(\text{nitrification rate}) = -0.8447(\log(O_2)^2 + 1.711 \log(O_2) + 0.7934$

253 There was also a significant linear negative correlation between the nitrification rate and NH_4^+
254 concentrations but the R-value (0.4262) was lower than for equation 2. No significant correlation was found
255 when both O_2 and NH_4^+ were included in to the analysis.

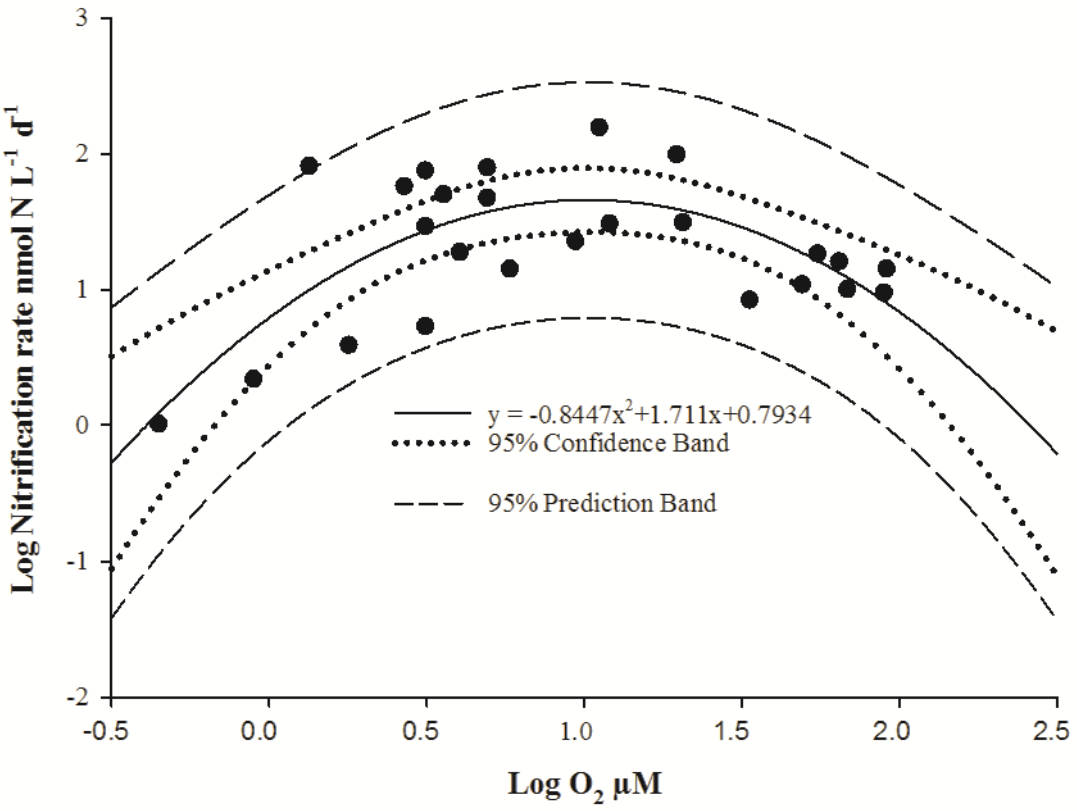

Figure 2. The regression model for nitrification rates in the Central Baltic Sea water column.

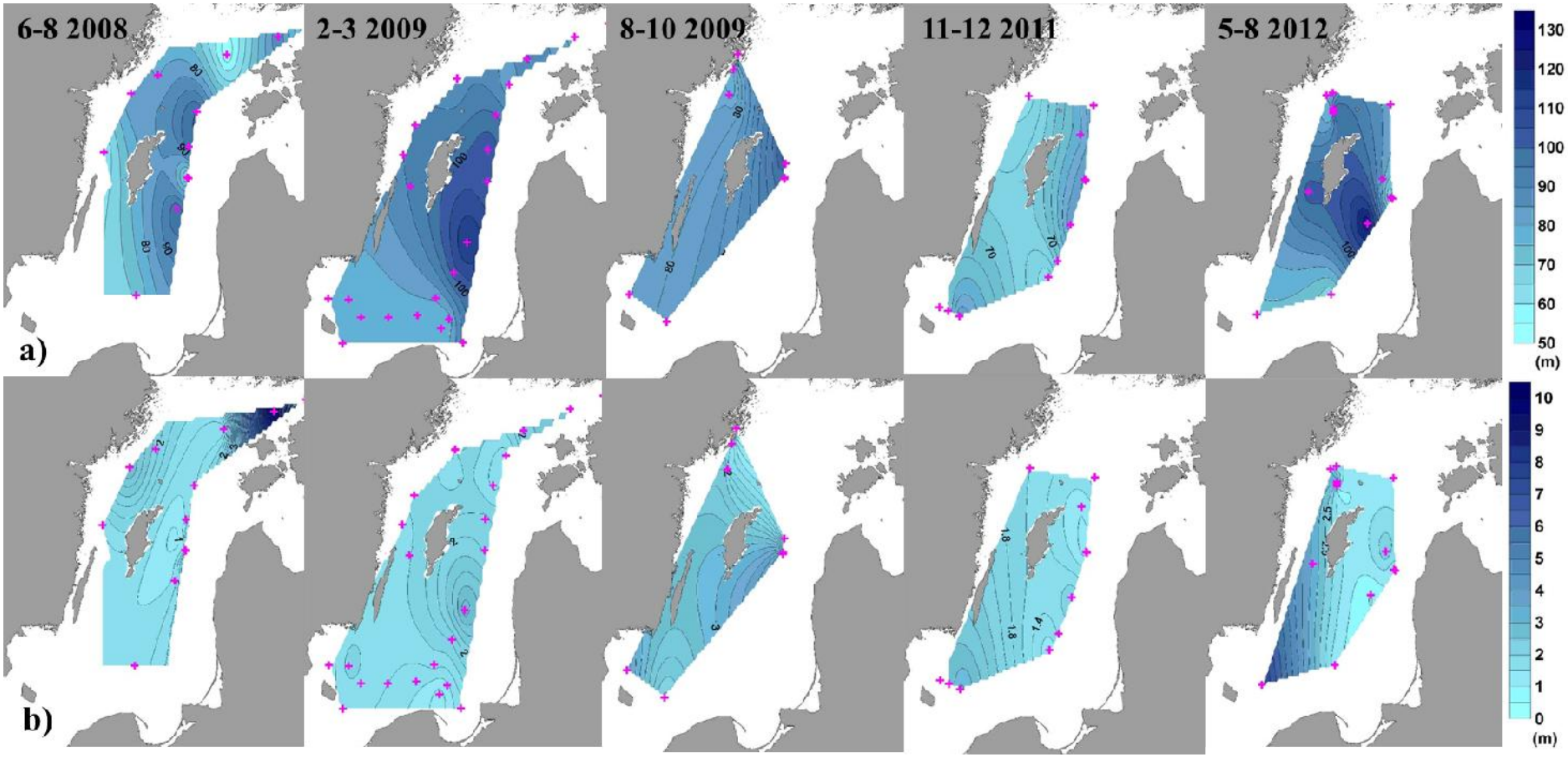

Figure 3. The depth of the center of the nitrification layer (a) and thickness (b) of the nitrification layer 2008-2012. Data was compiled from the IOW monitoring database.

The modeled nitrification rates in redoxclines were 39.9 ± 3.6 nmol N L^{-1} d^{-1} (2009), 38.5 ± 6.3 nmol N L^{-1} d^{-1} (2010), and 35.9 ± 11.7 nmol N L^{-1} d^{-1} (2011). The average depth of the modelled nitrification layer was 83 ± 18 m at GD, 77 ± 11 m at LD and 75.4 for F80 and the thickness of the nitrification layer varied between 0.86–3.11 m in the sampling stations (Figure 3, Table 2). There are no data available to compute the depth of the nitrification layer at GB1 and only one time point for F80 (Table 2). The area suitable for nitrification to proceed in the water column was approximately 77,540 ± 1000 km^2 and multiplying this area with the average thickness of the water layer suitable for nitrification (2.04± 1.40 m (Figure 4)), and the average nitrification rate from the equation, results an approximate annual amount of nitrification of 30.07±21.64 kt of N.

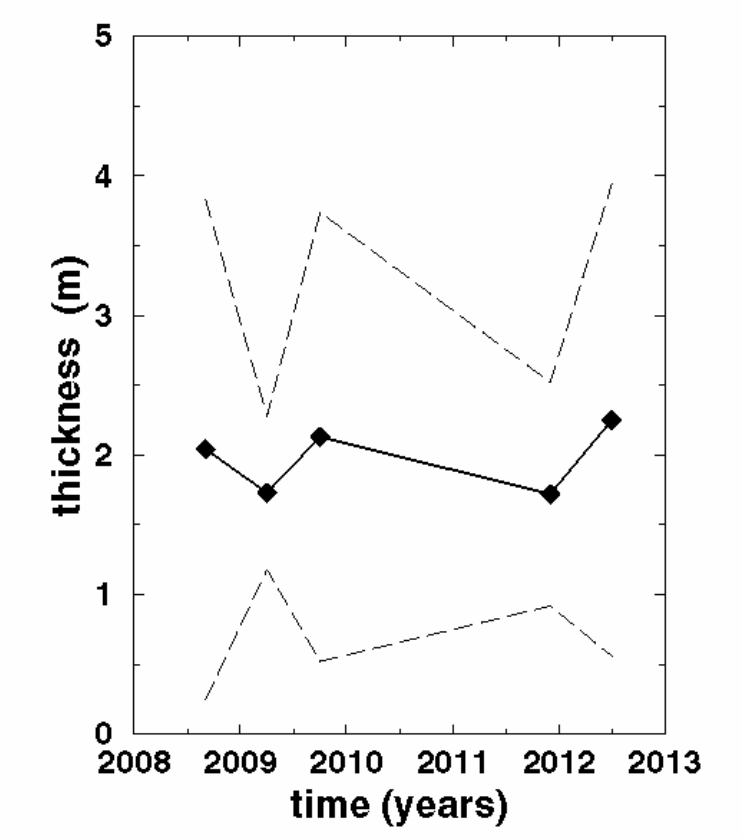

Figure 4. The average thickness and the standard deviation of nitrification layer in the central Baltic Sea 2008-2012.

Table 2. The depth/thickness of the nitrification layer (m) in 2008-2012 at GD, LD and F80. No data for GB1 is available in the IOW monitoring database.

	F80	**LD**	**GD**
6–8, 2008	N/A	85.40/2.88	59.41/1.19
2–3, 2009	N/A	N/A	99.51/1.95
8–10, 2009	N/A	77.58/2.19	92.54/2.87
11–12, 2011	75.36/1.01	62.79/1.60	80.36/0.86
5–8, 2012	N/A	81.69/3.11	83.17/2.46
AVERAGE	**75.36/1.01**	**76.87/2.46**	**83.00/1.87**
STD	**-**	**11.48/0.69**	**17.58/0.84**

3.3. Ammonia-oxidizing organism community composition

The Bray-Curtis dissimilarity index (0.05–0.19) for each replicate pairwise comparison indicated substantial variability between the replicates. However, the samples in general did cluster by pairs of replicates. For station GB1, only one sample was included for the AOB analysis, because the replicate sample did not hybridize well and the results were discarded. Overall, the archetypes for both AOA and AOB were quite evenly distributed (Figure 5) and the Shannon evenness index varied between 0.89 and 0.99 (Figure 5). The AOB and AOA communities at GB1 were the least even (Shannon evenness index 0.89), indicating that there were some archetypes that were relatively more important than others at this station.

For AOB, the highest signal archetype at GB1 as well as at LD was AOB16. The other important archetypes were AOB20 and AOB26 (Figure 5). For the AOA, there were three somewhat disproportionately important archetypes at all stations: AOA9, AOA12, and AOA4 (Figure 5). The RDA indicates that the AOB and AOA communities at GD clustered furthest away from the communities at GB1, whereas the communities at LD were located between GB1 and GD (Figure 6). The samples from the GD 123 m and 126 m were relatively similar indicating that although the potential nitrification rates declined, the ammonia oxidizer community did not change (Table 1, Figure 6). There was surprisingly wide variation between the replicate samples at LD; however, no errors were found in the analytical procedure, so both replicates were included in the analysis.

The AOB16 archetype was highly correlated with the potential nitrification rates and, therefore, with the samples from LD, where the rates were highest (Figure 6). If AOB are important at all in this system, this archetype is probably the most important, based on its high relative abundance and correlation with the potential nitrification rate. AOB7, AOB17, AOB20, AOB22, and AOB27 all showed their highest RFR signals at GB1, the sample that had the highest O_2 concentration (Figure 6). Hence, these archetypes were probably associated with higher O_2 concentrations. None of the other AOB archetypes showed any striking patterns. AOA4 and AOA12 showed the highest signals at GB1, while AOA9 showed high signals at both the GB1 and LD stations (Figure 5). AOA14 was correlated with potential nitrification rate and showed its highest signal in the first replicate at LD, but was moderate in the second. Hence, there was poor replication between the samples. AOA3 and AOA5 showed consistently high signals at both depths sampled at GD and were correlated with NH_4^+, which was highest at 126 m at GD (Figure 6).

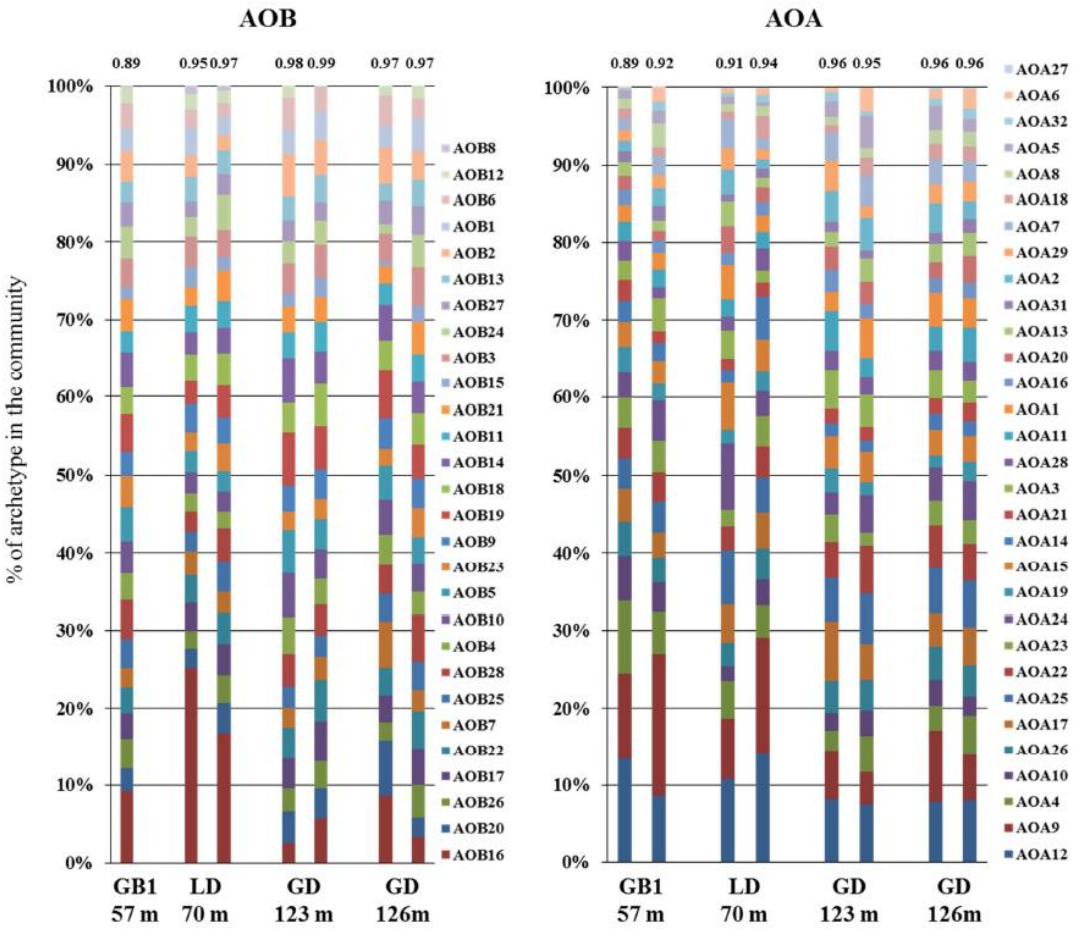

299 **Figure 5.** Distribution of archetypes based on relative fluorescence ratio (RFR) signals. The Shannon
300 evenness index is presented on top of the bars.

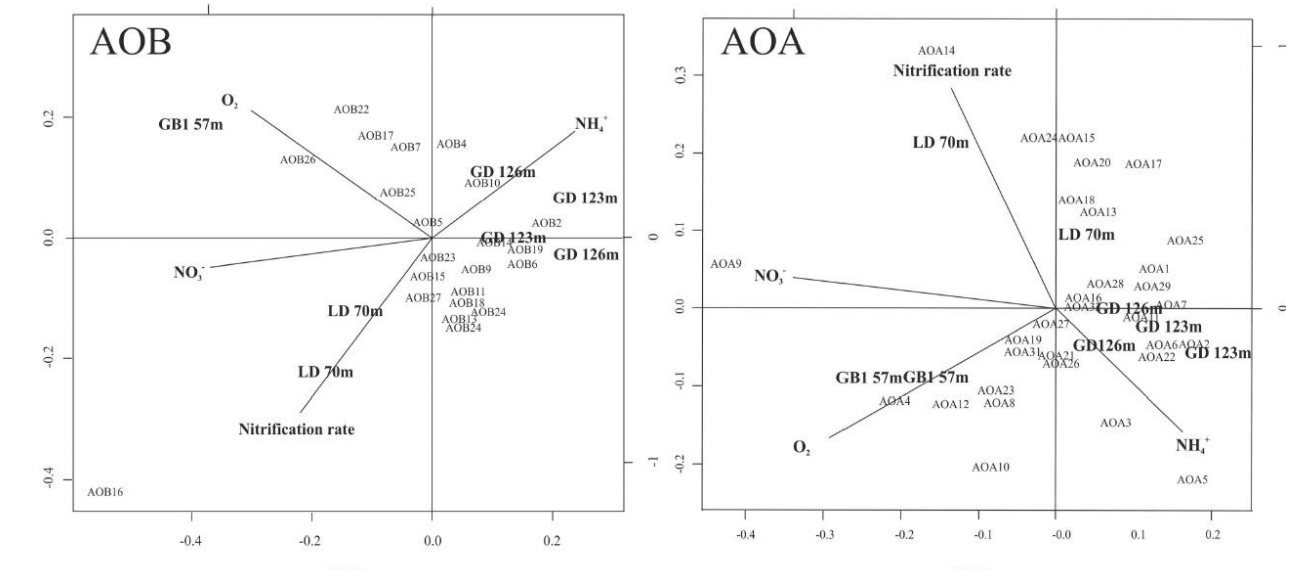

Figure 6. Redundancy analysis (RDA) maps of the AOB and AOA, sampling stations, and environmental parameters.

4. Discussion

4.1. Nitrification rates in the redoxclines

The potential nitrification rates measured in this study suggest that the maximal rates in the central Baltic Sea occur right above the oxic-anoxic interface and the rates decrease to zero quickly above and below that (Table 1). This was particularly demonstrated in the samples that were taken at LD in 2010. At 70 m the potential was at its highest but the rates quickly decreased below detection limit by 73 m, the depth where O_2 was not present anymore. However, at 76 m there was again O_2 and nitrification potential commenced above detection limit. Hence, it appears that nitrification does not only proceed in a uniform layer but also in lenses that contain O_2 below the oxic anoxic interface. The presence of O_2 at GD in 2010 fluctuated similar to LD, but nitrification did not initiate at 126 m although O_2 concentration increased slightly from 123 m. Hence,

the presence of nitrification at these lenses may be regulated also other factors than O_2, such as proximity of H_2S, which is known to inhibit nitrification in the pelagic Baltic Sea (Berg *et al.* 2015).

The calculated water layer where conditions are favorable for nitrification is surprisingly narrow and there was very little variation between the areas and years (Figure 3, Figure 4). We always tried to target the most active nitrification layer based on the inspection of O_2 profile, yet the rates were often below detection limit or very low, indicating that we may have missed the most active layer (Table 1). When Labrenz *et al.* (2010) measured the ammonia oxidizer gene expression they found, similar to us, the highest activity in a two meters thick water layer at the oxic anoxic boundary. The reason for the thin nitrification layer in the Baltic Sea is probably the lack of extended suboxic zone where conditions are favorable for pelagic nitrification (Lam *et al.* 2007, Lam *et al.* 2009, Kalvelage *et al.* 2011, Bristow *et al.* 2016) and which is a prominent feature of many other ODZs such as the Black Sea (Yakushev *et al.* 2008), the Eastern Tropical Pacific OMZ's (Paulmier *et al.* 2006) and the Saanich Inlet (Zaikova *et al.* 2009). The narrow suboxic layer is also consistent with very low anammox and N_2O production rates in the Baltic Sea. Anammox is inhibited by H_2S and it occurs at significant rates in the Baltic Sea only after inflows when H_2S has not reached the suboxic layer (Hannig *et al.*, 2007, Bonaglia *et al.*, 2016). Similarly, substantial N_2O formation, which results from nitrification in suboxic conditions, has been found only after inflows when sulfidic waters have not reached the oxic anoxic interface (Myllykangas *et al.,* 2017). Observations in the Bornholm Basin in the southern Baltic Sea (van der Lee and Umlauf, 2011) indicate that higher modes of the near-inertial wave spectrum are generated at the slope of the basin and they create persistent narrow shear band. These perturbations propagate in to the EGB from the edge of the basin into its interior at the redoxcline (Holtermann *et al.*, 2017). The narrow bands of high shear are directly associated with narrow bands of dissipation, the major source of turbulent mixing (Lappe and Umlauf, 2016) that prevents the formation of the thick suboxic layer. This also explains the formation of O_2 containing lenses, which harbors nitrification below the oxic anoxic interface.

The depth of the nitrification layer was between 59–100 m in at GD and 63–85 m at LD. Hence, the depth of the nitrification layer varied more at GD (Figure 3, Table 2). Although there were no MBIs during the analysis period, the position of the nitrification layer appears to fluctuate substantially particularly in the EGB (Figure 3). The dynamic nature of the nitrification layer in this area may be explained by minor inflows that occurred during the analysis period (Naumann *et al*., 2016). The minor inflows are not strong enough to replace old anoxic water in the bottom of the basins. Instead, they mix with the intermediate water layers and cause entrainment of the water column. The minor inflows propagate first into the EGB before traveling into the WGB. As the inflowing water travels through the EGB, its salinity decreases when the water masses mix with less saline water. Consequently, the inflow weakens and may not necessarily reach the WGB at all. Therefore, WGB has less frequent and weaker lateral intrusions and a more stable redoxcline (Matthäus *et al*., 2008), which also appears to cause the depth of the nitrification layer to remain more stable (Figure 3, Table 2).

4.2. Nitrification as a regulatory factor for nitrogen removal in the Baltic Proper redoxclines

Denitrification is an important sink for NO_x^- in the central Baltic Sea and it has been estimated to remove 132–547 kton N yr^{-1} (Dalsgaard *et al.,* 2013). We estimated that nitrification produces approximately 30 kton of N yr^{-1}, which is less than a quarter of the lowest denitrification estimate. In order for nitrification to match the denitrification rates estimated by Dalsgaard *et al*., (2013) the average nitrification rate at the entire central Baltic Sea would have to be approximately 170 nmol N L^{-1} d^{-1} which still is within the 95% prediction interval of the regression model (Figure 2). Such high rates have also been measured in the area (Hietanen *et al*., 2012), but based on our measurements and model, they are unlikely to be maintained throughout the year in the entire area. Hence, although there is a strong coupling between nitrification and denitrification in the central Baltic Sea (Frey *et al*., 2014), there are probably additional sources of NO_3^- for denitrification. Such sources could be nitrification occurring in lenses formed by mixing and lateral transport

of NO_3^- by advection. However, their importance as NO_3^- source for denitrification needs further investigations.

4.3. Community composition of ammonia-oxidizing organisms in the central Baltic Sea

The high signals for AOB16 and AOB20 were consistent with the origin of these archetype sequences and the characteristics of the Baltic environment. The archetype sequence of AOB16 is from Kysings Fjord, a small coastal lagoon in Denmark (Nicolaisen and Ramsing, 2002). Kysings Fjord is characterized by high N loads, salinity of 14, and virtually no tidal action (Nielsen *et al.*, 1995). This archetype was also associated with high potential nitrification rates, so the most active AOB in the Baltic Sea probably cluster closely with this archetype. The sequence of AOB20 is based on *N. cryotolerans*, which was originally isolated from cold waters in Alaska and is capable of growth even at temperatures of -5 °C (Jones *et al.*, 1988). Although the temperature in the sampling depth was cool (~5 °C), the appearance of this archetype is not necessarily tied to temperature, since the archetype is universally distributed. For example, this sequence was retrieved in a wastewater treatment plant in Japan (Limpiyakorn *et al.*, 2005). The rarer archetype among the highest signals was AOB26 (Figure 5). This archetype sequence was derived from Gulf of Finland sediments located in the northern Baltic Sea and it has been detected elsewhere (e.g. Chesapeake Bay, Bouskill *et al.*, 2011), but not as a major component of the assemblage. Therefore, the high relative abundance of AOB26 seems to be specific for the Baltic Sea and is in line with the results of Vetterli *et al.*, (2016) indicating that the Baltic Sea harbors unique ammonia oxidizer sequences.

The AOA microarray results showed no striking patterns specific for the Baltic Sea. Similar high relative abundances for AOA9, AOA12, and AOA4 have been shown in other studies in which AOA microarrays were applied for marine samples (Bouskill *et al.*, 2012, Newell *et al.*, 2013). The sequence for AOA9 was derived from deep low-O_2 water samples from the Gulf of California and has also been detected in deep

385 water from Monterey Bay and off Hawaii at station ALOHA. While the Baltic Sea redoxcline, too, shows
386 low O_2 conditions, the Baltic Sea is relatively shallow, and the low O_2, rather than depth, appears to regulate
387 the presence of this archetype. The sequence for archetype AOA12 was compiled from sequences derived
388 primarily from representatives of Tobari sediments, a hypernutrified estuary in Mexico, and from clones that
389 are derived from soil. The sequence for AOA4 was derived from *N. gargensis* and sequences representing
390 soil and sediment. Although AOA12 and AOA4 were associated with soil and sediment, these archetypes are
391 also commonly found in marine water columns (Bouskill *et al.*, 2012; Newell *et al.*, 2013). Interestingly, the
392 high relative abundance of these three archetypes appears not to be dependent on salinity, because they have
393 been found under completely marine conditions (Newell *et al.*, 2013), as well as the brackish water
394 conditions that were present in this study.

395 AOA1 was not among the archetypes that showed high signal strength (Figure 5), although its probe
396 sequence is derived from *N. maritimus* and should be closely related to AOA cluster GD2, detected at high
397 abundance in the Baltic by Labrenz *et al.* (2010) and Berg *et al.* (2015). This suggests that the GD2 cluster
398 a*moA* sequences did not hybridize with the AOA1 probe because the sequence fragments published by
399 Labrenz *et al.* (2010) only partially overlap with the AOA1 probe sequence and that GD2 is not closely
400 related to *N. maritimus.* The GD2 *amoA* sequence appears to be only about 90% identical to the AOA1 probe
401 sequence and this degree of similarity between target and probe would produce low signals even if the
402 mismatched target were abundant. Hence, it appears that the dominant thaumarchaeotal subcluster in the
403 Baltic Sea has evolved a unique lineage that is adapted to the varying salinity, and O_2 and H_2S
404 concentrations. If the GD2 sequence had been available at the time of the array design, it probably would
405 have constituted a distinct new archetype probe, the inclusion of which in the microarray could have shifted
406 the diversity of the AOA archetypes to a less even distribution. Nevertheless, the comparisons are made on
407 the basis of relative contribution to the assemblages in different samples and their relationship to
408 environmental variables remain valid.

4.4. Effect of water column hydrodynamics on nitrifying communities

In microarray analyses, the number of types detected is limited by the number of probes; hence the diversity index (number of species) is not a proper measure of diversity. Instead, the evenness index should be used. In this study, the overall species evenness was higher than anywhere else where ammonia oxidizer assemblages have been analyzed using a similar method (Ward *et al*., 2007; Bouskill *et al*., 2011, 2012; Newell *et al*., 2013). The high degree of evenness in the AOA and AOB communities may be explained by the unique physical features of the Baltic Sea that cause disturbances to the water layers where ammonia oxidizers are present. The intermittently occurring MBIs and the frequent turbulent mixing in the redoxcline causes variation in salinity, which has been suggested to be one of the main drivers for the diversity of ammonia oxidizers (Bernhard *et al.* 2005). Mixing also alters the geochemistry, which is a major driver for the OTU distribution (Bouskil *et al.* 2012). Mixing of the water column is more prominent in the EGB than in the WGB (Matthäus *et al*., 2008, Dellwig *et al*., 2012, Jakobs *et al*., 2013) (Figure 3) and the more stable redoxcline at GB1 may allow the most adapted species to dominate the ammonia oxidizer community, which is consistent with the less even distribution of archetypes at that station.

Physical processes, such as turbulence and advection, control salinity and the distribution of geochemical components. Since salinity and geochemical components are highly correlated with the compositions and activity levels of microbial communities, they also govern the biological cycling of geochemical components. This study is a modest attempt to demonstrate this and in the changing climate, even more thorough combination of biological and hydrodynamic data is required in order to understand the future projections of the biogeochemical cycles.

Conclusions

The nitrification rates in the central Baltic Sea are at their highest in the upper redoxcline and quickly decrease below detection limit a few meters below and above the most active layer. This is caused by the lack of an extensive suboxic zone, which is a prominent feature of many other ODZs. There is very little temporal variation in the average nitrification rates and the average thickness of the nitrification layer. The limited size of the persistent nitrification layer might be directly associated to the turbulent mixing. Higher modes of near-inertial gravity waves create narrow bands of high shear and dissipation and such a permanent physical forcing seems to be sufficient to form the thin and persistent nitrification layer. However, the depth of the water layer where conditions are suitable for nitrification had more variability in the EGB than in the WGB. The thin nitrification layer highlights the uniqueness of the hydrodynamics in the Baltic Sea and its effects on the nitrification rates – the volumetric rates are some of the highest measured pelagic redoxclines, yet the areal rates are low because the conditions favourable for nitrification are found only in a narrow water layer. The turbulent conditions in the redoxcline also seem govern the ammonia-oxidizing community composition because the community is more evenly distributed than observed elsewhere where functional micro-arrays have been applied. The ammonia-oxidizing community in the EGB is more even than in the WGB and the reason for the more even community composition is most likely the more dynamic redoxcline where environmental conditions change constantly, allowing no predominance of single ammonia-oxidizing archetype.

Funding and Conflicts of interest

The work was supported by the BONUS + projects HYPoxia mitigation for Baltic Sea Ecosystem Restoration (HYPER); Assessment and Modelling of Baltic Ecosystem Response (AMBER); the Finnish doctoral programme in Environmental Science and Technology (EnSTe), and Academy of Finland (grant number 139267). None of the authors have conflict of interest.

Acknowledgements

We acknowledge Maren Voss from the Baltic Sea Research Institute in Warnemünde (IOW) for organizing the sampling cruises and we thank Emila Röhr (University of Helsinki) and the crews of R/V Heincke, R/V Pelagia, R/V Elisabeth Mann Borgese for all their help during the sample collection. We are indebted to Lars Umlauf (IOW) for helpful comments and discussions about the hydrodynamics of the Baltic Sea. We thank Iris Liskow (IOW) and Birgit Sadkowiak (IOW) for help with the nutrient analyses, Claudia Frey (IOW) for organizing the data, and Caroline Möller (IOW) and Katja Käding (IOW) for support with the molecular biological data base. Christina Biasi and Simo Jokinen from the University of Eastern Finland, Department of Environmental Science, were an invaluable aid during the stable isotope analyses.

References

Bauer S. Structure and function of nitrifying bacterial communities in the Eastern Gotland Basin (Central Baltic Sea). PhD thesis, University of Rostock, Rostock, 2003.

Berg G, Vandieken V, Thamdrup B, Jürgens K. Significance of archaeal nitrification in hypoxic waters of the Baltic Sea. *ISME J* 2015, DOI: 10.1038/ismej.2014.218.

Bernhard AE, Donn T, Giblin AE, *et al.* Loss of diversity of ammonia-oxidizing bacteria correlates with increasing salinity in an estuary system. *Environmental Microbiology* 2005, DOI: 10.1111/j.1462-2920.2005.00808.x

Bonaglia S, Klawonn I, De Brabandere L, *et al.* Denitrfication and DNRA at the Baltic Sea oxic-anoxic interface: Substrate spectrum and kinetics. Limnol Oceanogr 2016, DOI:10.1002/lno.10343.

Bouskill NJ, Eveillard D, O'Mullan G, *et al*. Seasonal and annual reoccurrence in betaproteobacterial ammonia-oxidizing bacterial population structure. *Environ Microbiol* 2011, DOI: 10.1111/j.1462-2920.2010.02362.x.

Bouskill NJ, Eveillard D, Chien D, *et al.* Environmental factors determining ammonia-oxidizing organism distribution and diversity in marine environments. *Environ Microbiol* 2012, DOI: 10.1111/j.1462-2920.2011.02623.x.

Brettar I, Rheinheimer G. Denitrification in the central Baltic – evidence for H_2S-oxidation as motor of denitrification at the oxic–anoxic interface. *Mar Ecol Prog Ser*, 1991;**77**: 157–169.

Bristow LA, Dalsgaard T, Tiano L, *et al*. Ammonium and nitrite oxidation at nanomolar oxygen concentrations in oxygen minimum zone waters. *Proc Natl Acad Sci USA* 2016, DOI: 10.1073/pnas.1600359113.

Brochier-Armanet C, Boussau B, Gribaldo S, *et al*. Mesophilic crenarchaeota: proposal for a third archaeal phylum, the Thaumarchaeota. *Nat Rev Microbiol* 2008, DOI: 10.1038/nrmicro1852.

Bulow SE, Francis CA, Jackson GA *et al*. Sediment denitrifier community composition and *nirS* gene expression investigated with functional gene microarrays. *Environ Microbiol* 2008, DOI: 10.1111/j.1462-2920.2008.01765.x.

Codispoti LA, Brandes JA, Christensen JP, *et al*. The oceanic fixed nitrogen and nitrous oxide budgets: Moving targets as we enter the anthropocene? *Scientia Marina* 2001, DOI: 10.3989/scimar.2001.65s285.

Daims H, Lebedeva EV, Pjevac P, *et al*. Complete nitrification by *Ntrospira* bacteria. *Nature* 2015, DOI: 10.1038/nature16461.

Dalsgaard T, De Brabandere L, Hall POJ. Denitrification in the water column of the central Baltic Sea. *Geochim Cosmochim Acta* 2013, DOI:10.1016/j.gca.2012.12.038.

Dellwig O, Schnetger B, Brumsack *et al*. Dissolved reactive manganese at pelagic redoxclines (part II): Hydrodynamic conditions for accumulation, *J Mar Syst* 2012, DOI: 10.1016/j.jmarsys.2011.08.007

Enoksson V. Nitrification rates in the Baltic Sea: comparison of three isotope techniques. *Appl Environ Microbiol* 1986;**51**: 244–250.

Frey C, Dippner JW, Voss M. Close coupling of N-cycling processes expressed in stable isotope data at the redoxcline of the Baltic Sea. *Global Biogeochem. Cycles,* 2014. DOI: 10.1002/2013GB004642.

Grasshoff K, Kremling K, Ehrhardt M. Methods of Seawater Analysis, 2nd ed. Weinheim: Verlag Chemie GmbH, 1983.

Grundle DS, Juniper SK. Nitrification from the lower euphotic zone to the sub-oxic waters of a highly productive British Columbia fjord. *Marine Chemistry*, 2011, DOI: 10.1016/j.marchem.2011.06.001

Hannig M, Lavik G, Kuypers MMM *et al*. Shift from denitrification to anammox after inflow events in the central Baltic Sea. *Limnol Oceanogr* 2007, DOI: 10.4319/lo.2007.52.4.1336.

HELCOM. Eutrophication in the Baltic Sea: An integrated thematic assessment of the effects of nutrient enrichment in the Baltic Sea region. Baltic Sea Environment Proceedings No. 115B. 2009.

Hietanen S, Jäntti H, Buizert C, *et al*. Hypoxia and nitrogen processing in the Baltic Sea water column. *Limnol Oceanogr* 2012, DOI: 10.4319/lo.2012.57.1.0325.

Holtermann PL, Prien R, Naumann M *et al*. Deep-water dynamics and mixing processes during a major inflow event in the central Baltic Sea. *J Geophys Res: Oceans* 2017, DOI: 10.1002/2017JC013050.

Jakobs G, Rehder G, Jost G, *et al*. Comparative studies of pelagic microbial methane oxidation within the redox zones of the Gotland Deep and Landsort Deep (central Baltic Sea). *Biogeosciences* 2013, DOI: 10.5194/bg-10-7863-2013.

Jones RD, Morita RY, Koops HP, *et al*. A new marine ammonium-oxidizing bacterium, *Nitrosomonas cryotolerans* sp. nov. *Can J Microbiol* 1988, DOI: 10.1139/m88-198.

519 Jäntti H, Jokinen S, Hietanen S. Effect of nitrification inhibitors on the Baltic Sea ammonia-oxidizing
520 community and precision of the denitrifier method. *Aquat Microb Ecol* 2013, DOI: 10.3354/ame01653.

521 Kalvelage T, Jensen MM, Contreras S, *et al*. Oxygen sensitivity of anammox and coupled N-cycle processes
522 in oxygen minimum zones. *PloS one* 2011, DOI: 10.1371/journal.pone.0029299.

523 Kuzmina N, Rudels B, Stipa T, *et al*. The structure and driving mechanisms of the Baltic intrusions. *J. Phys.*
524 *Oceanogr* 2005, DOI:10.1175/JPO2749.1.

525 Könneke M, Bernhard AE, de la Torre JR, *et al*. Isolation of an autotrophic ammonia-oxidizing marine
526 archaeon. *Nature* 2005, DOI: 10.1038/nature03911.

527 Labrenz M, Sintes E, Toetzke F, *et al*. Relevance of a crenarchaeotal subcluster related to *Candidatus*
528 *Nitrosopumilus maritimus* to ammonia oxidation in the suboxic zone of the central Baltic Sea. *ISME J* 4
529 2010, DOI: 10.1038/ismej.2010.78.

530 Lappe C, Umlauf L. Efficient boundary mixing due to near-inertial waves in a nontidal basin: Observations
531 from the Baltic Sea. *J Geophys Res: Oceans*, 2016. DOI: 10.1002/2016JC011985.

532 Lam P, Jensen MM, Lavik G, *et al*. Linking crenarchaeal and bacterial nitrification to anammox in the Black
533 Sea. *Proc Natl Acad Sci USA*, 2007, DOI: 10.1073/pnas.0611081104.

534 Lam P, Lavik G, Jensen MM, *et al*. Revising the nitrogen cycle in the Peruvian oxygen minimum zone. *Proc*
535 *Natl Acad Sci USA* 2009, DOI: 10.1073/pnas.0812444106.

536 Limpiyakorn T, Shinohara Y, Kurisu F *et al*. Communities of ammonia-oxidizing bacteria in activated
537 sludge of various sewage treatment plants in Tokyo. *FEMS Microbiol Ecol* 2005, DOI:
538 10.1016/j.femsec.2005.03.017

539 Matthäus W, Nehring D, Feistel R, *et al*. The Inflow of Highly Saline Water into the Baltic Sea. State and
540 Evolution of the Baltic Sea. In: Feistel R, Nausch G, Wasmund N (Eds), 1952-2005: A Detailed 50-Year
541 Survey of Meteorology and Climate, Physics, Chemistry, Biology, and Marine Environment. John Wiley &
542 Sons, Inc., Hoboken, NJ, USA pp. 265-310, 2008, DOI: 10.1002/9780470283134.ch10

543 Myllykangas JP, Jilbert T, Jakobs G, *et al*. Effects of the 2014 major Baltic inflow on methane and nitrous
544 oxide dynamics in the water column of the central Baltic Sea. *Earth System Dynamics* 2017, DOI:
545 10.5194/esd-8-817-2017.

546 Naumann M, Günther Nausch G, Mohrholz V. 2016. Water Exchange between the Baltic Sea and the North
547 Sea, and conditions in the Deep Basins. HELCOM Baltic Sea Environment Fact Sheets. Online. 30.6.2017.
548 http://www.helcom.fi/baltic-sea-trends/environment-fact-sheets/.

549 Newell SE, Fawcett SE, Ward BB. Depth distribution of ammonia oxidation rates and ammonia-oxidizer
550 community composition in the Sargasso Sea. *Limnol Oceanogr* 2013, DOI: 10.4319/lo.2013.58.4.1491.

551 Nicolaisen MH, Ramsing NB. Denaturing gradient gel electrophoresis (DGGE) approaches to study the
552 diversity of ammonia-oxidizing bacteria. *J Microbiol Methods* 2002, DOI: 10.1016/S0167-7012(02)00026-
553 X.

554 Nielsen K, Nielsen LP, Rasmussen P. Estuarine nitrogen retention independently estimated by the
555 denitrification rate and mass balance methods: a study of Norsminde Fjord, Denmark. *Mar Ecol Prog Ser*
556 1995;**119**: 275–283.

557 Paulmier A, Ruiz-Pino D, Garçon V *et al*. Maintaining of the Eastern South Pacific oxygen minimum zone
558 (OMZ) off Chile. *Geophysical Research Letters* 2006, DOI: 10.1029/2006GL026801.

559 Reissmann J, Burchard H, Feistel R, *et al*. State-of-the-art review on vertical mixing in the Baltic Sea and
560 consequences for eutrophication. *Progr Oceanogr* 2009, DOI: 10.1016/j.pocean.2007.10.004.

561 Rönner U. Distribution, production and consumption of nitrous oxide in the Baltic Sea. *Geochim Cosmochim*
562 *Acta* 1983, DOI: 10.1016/0016-7037(83)90041-8.

563 Rönner U, Sörensson F. Denitrification rates in the low oxygen waters of the stratified Baltic proper. *Appl*
564 *Environ Microbiol* 1985;**50**: 801–806.

565 Schinke H, Matthäus W. On the causes of major Baltic inflows —an analysis of long time series. *Cont Shelf*
566 *Res* 1998, DOI: 10.1016/S0278-4343(97)00071-X.

567 Schloss PD, Handlesman J. Introducing DOTUR, a computer program for defining operational taxonomic
568 units and estimating species richness. *Appl Environ Microbiol* 2005, DOI: 10.1128/AEM.71.3.1501-1506.

569 Sigman DM, Casciotti KL, Andreani M, et al. A bacterial method for the nitrogen isotopic analysis of nitrate
570 in seawater and freshwater. *Anal Chem* 2001, DOI: 10.1021/ac010088e.

571 Taroncher-Oldenburg G, Griner EM, Francis CA *et al*. Oligonucleotide microarray for the study of
572 functional gene diversity in the nitrogen cycle in the environment. *Appl Environ Microbiol* 2003, DOI:
573 10.1128/AEM.69.2.1159-1171.2003.

574 van der Lee EM, Umlauf, L. Internal wave mixing in the Baltic Sea: Near-inertial waves in the absence of
575 tides. *J Geophys Res: Oceans* 2011, DOI: 10.1029/2011JC007072.

576 Vetterli A, Hietanen S, Leskinen E. Spatial and temporal dynamics of ammonia oxidizers in the sediments of
577 the Gulf of Finland, Baltic Sea. *Mar Environ Res* 2016, DOI: 10.1016/j.marenvres.2015.12.008.

578 Ward BB, Eveillard D, Kirshtein JD, *et al*. Ammonia-oxidizing bacterial community composition in
579 estuarine and oceanic environments assessed using a functional gene microarray. *Environ Microbiol* 2007,
580 DOI: 10.1111/j.1462-2920.2007.01371.x.

581 Ward BB, Bouskill NJ. The utility of functional gene arrays for assessing community composition, relative
582 abundance, and distribution of ammonia-oxidizing bacteria and archaea. *Method Enzymol* 2011;**496**: 373–
583 396.

584 Yakushev E, Chasovnikov V, Murray J, *et al*. Vertical hydrochemical structure of the Black Sea. In:
585 Kostianoy AG, Kosarev AN (eds). The Black Sea Environment, Vol 5Q Springer: Berlin/Heidelberg, pp.
586 277–307, 2008.

587 Zaikova E, Walsh DA, Stilwell CP, *et al*. Microbial community dynamics in a seasonally anoxic fjord:
588 Saanich Inlet, British Columbia. *Environ Microbiol*, 2010. DOI: 10.1111/j.1462-2920.2009.02058.x

589 Zhurbas VM, Paka VT. What drives thermohaline intrusions in the Baltic Sea? *J Mar Syst* 1999, DOI:
590 10.1016/S0924-7963(99)00016-0.